Table 2. Clinicopathologic features of the patients

	Training set								Test set					
	Biopsy sample				Washing fluid				Biopsy sample			Washing fluid		
	IT ($n = 52$)	NI ($n = 98$)	*P*	Normal ($n = 187$)	IT ($n = 36$)	NI ($n = 34$)	*P*	Normal ($n = 18$)	IT ($n = 20$)	NI ($n = 21$)	*P*	IT ($n = 23$)	NI ($n = 24$)	*P*
Demographics														
Age	67.4	66.7	0.720	67.2	68.8	64.7	0.101	59.6	69.3	69.6	0.553	70.3	69.3	0.707
Male	16 (30.8%)	24 (24.5%)		126 (67.4%)	22 (61.1%)	25 (73.5%)		9 (50.0%)	14 (70%)	14 (66.7%)		14 (60.9%)	17 (70.8%)	
Female	36 (69.2%)	74 (75.5%)	0.408	61 (32.6%)	14 (38.9%)	9 (26.5%)	0.269	9 (50.0%)	6 (30%)	7 (33.3%)	0.332	9 (39.1%)	7 (29.2%)	0.213
Tumor size														
≥25 mm	31 (59.6%)	12 (12.2%)			27 (75%)	5 (14.7%)			15 (75%)	3 (14.3%)		18 (78.3%)	3 (12.5%)	
<25 mm	21 (40.4%)	86 (87.8%)	<0.001		9 (25%)	29 (85.3%)	<0.001		5 (25%)	18 (85.7%)	<0.001	5 (21.7%)	21 (87.5%)	<0.001
Location														
Right	21 (40.4%)	44 (44.9%)			12 (33.3%)	17 (50%)			11 (55%)	12 (57.1%)		11 (47.8%)	13 (54.2%)	
Left	15 (28.8%)	25 (25.5%)			14 (38.9%)	7 (20.6%)			7 (35%)	7 (33.3%)		8 (34.8%)	8 (33.3%)	
Rectum	16 (30.8%)	29 (29.6%)	0.853		10 (27.8%)	10 (29.4%)	0.332		2 (10%)	2 (9.5%)	0.883	4 (17.4%)	3 (12.5%)	0.980
Histology														
Hyper/inflammatory		15 (15.3%)				3 (8.8%)				0 (0.0%)			0 (0.0%)	
Tubular adenoma		29 (29.6%)				10 (29.4%)				9 (42.9%)			12 (50%)	
Tubulovillous adenoma		28 (28.6%)				7 (20.6%)				7 (33.3%)			7 (29.2%)	
Severe dysplasia		26 (26.5%)				14 (41.2%)				5 (23.8%)			5 (20.8%)	
Cancer	52 (100.0%)				36 (100.0%)				20 (100.0%)			23 (100.0%)		

Abbreviations: IT: invasive tumors, NI: noninvasive tumors.

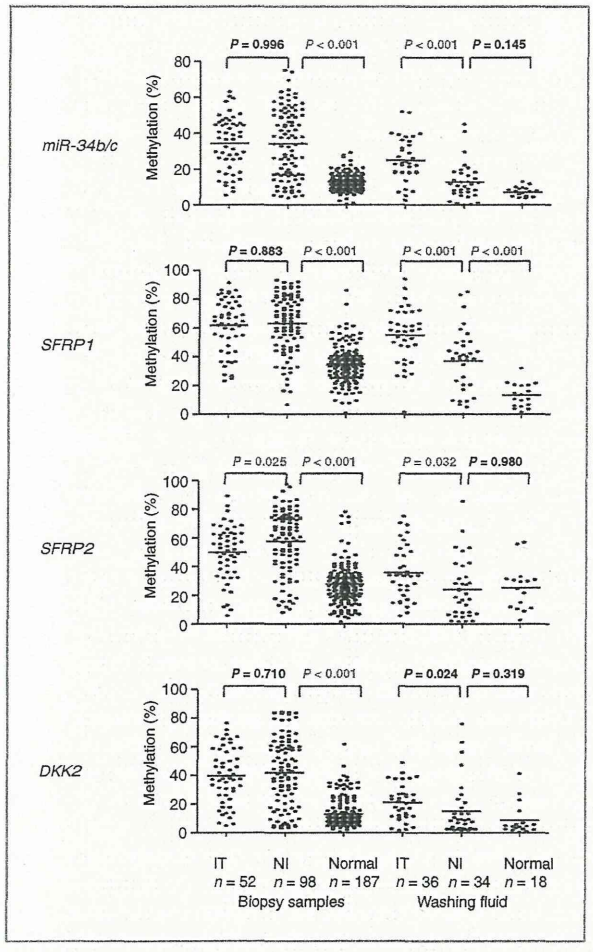

Figure 1. Levels of *mir-34b/c*, *SFRP1*, *SFRP2*, and *DKK2* methylation in invasive and noninvasive colorectal tumors. Methylation levels detected with DNA from biopsy and wash fluid. The genes analyzed are shown on the left.

sensitivity was observed (0.740, 17/23), the specificity was very high (0.958, 21/24). The total accuracy of the diagnosis was 85.1% (40/47) for the test set.

We also assessed the correlation between methylation levels detected in biopsy specimens and in wash fluid (Supplementary Fig. S2). We found that overall methylation levels in biopsy tissues and washing fluid were well correlated. When we divided the data for invasive and noninvasive tumors, however, only invasive tumors showed a significant correlation between methylation levels in biopsy tissue and washing fluid.

Detection of *K-ras* mutation by mucosal washing fluid

Finally, we tested for mutation of *K-ras* codons 12 and 13 by using DNA obtained from biopsy tissue or wash fluid (Supplementary Table S2). With invasive tumors, mutations of *K-ras* were found in 9 of 27 (33.3%) biopsy specimens. Among the 9 positive tumors, we were able to also detect mutations in 7 (77.7%) wash fluid samples. With noninvasive tumors, mutations were detected in 6 of 24 (25%) biopsy specimens, but in only 2 (33.3%) of the corresponding wash fluid samples. Addition of *K-ras* mutation did not improve the accuracy of diagnosis of invasiveness by the diagnostic tree (data not shown). Consistent with this finding, nuclear staining showed more intact nuclei in wash fluid from invasive tumors than from noninvasive tumors (Supplementary Fig. S1C). Thus, samples from invasive tumors seem to contain higher concentrations of tumor-derived DNA than samples from noninvasive tumors.

Discussion

Small colorectal tumors are usually removed by endoscopic mucosal dissection, but if the tumor is invasive, surgical treatment is required because of the higher risk of lymph node metastasis. Consequently, precise preoperative diagnosis is critical for appropriate treatment of colorectal tumors. Magnifying colonoscopy is a useful means of distinguishing invasive from noninvasive tumors (9, 10).

Table 3. Results of ROC analyses of the methylation levels in 4 genes in the training set.

Tumor size	Training set					
	Genes	AUC Estimate (95% CI)	Cutoff (%)	Sensitivity Estimate (95% CI)	Specificity Estimate (95% CI)	ORs Estimate (95% CI)
Total	*miR34b/c*	0.796 (0.686–0.906)	13.0	0.861 (0.705–0.953)	0.647 (0.465–0.803)	11.4 (3.5–36.9)
			17.8	0.833 (0.609–0.899)	0.765 (0.588–0.893)	16.3 (5.0–53.0)
			21.0	0.611 (0.435–0.769)	0.882 (0.726–0.967)	11.8 (3.4–40.7)
	SFRP1	0.736 (0.616–0.857)	45.0	0.750 (0.578–0.879)	0.706 (0.525–0.849)	7.2 (2.5–20.7)
	SFRP2	0.688 (0.562–0.814)	33.0	0.583 (0.408–0.745)	0.765 (0.588–0.893)	4.5 (1.6–12.8)
	DKK2	0.702 (0.572–0.831)	11.0	0.806 (0.64–0.918)	0.647 (0.465–0.803)	7.6 (2.6–22.5)
≥25mm	*miR34b/c*	0.816 (0.665–0.967)	15.0	0.862 (0.683–0.961)	0.667 (0.223–0.957)	12.5 (1.7–92.3)
<25mm	*SFRP1*	0.810 (0.594–1.000)	51.0	0.821 (0.631–0.939)	0.833 (0.359–0.996)	23.0 (2.2–242.1)

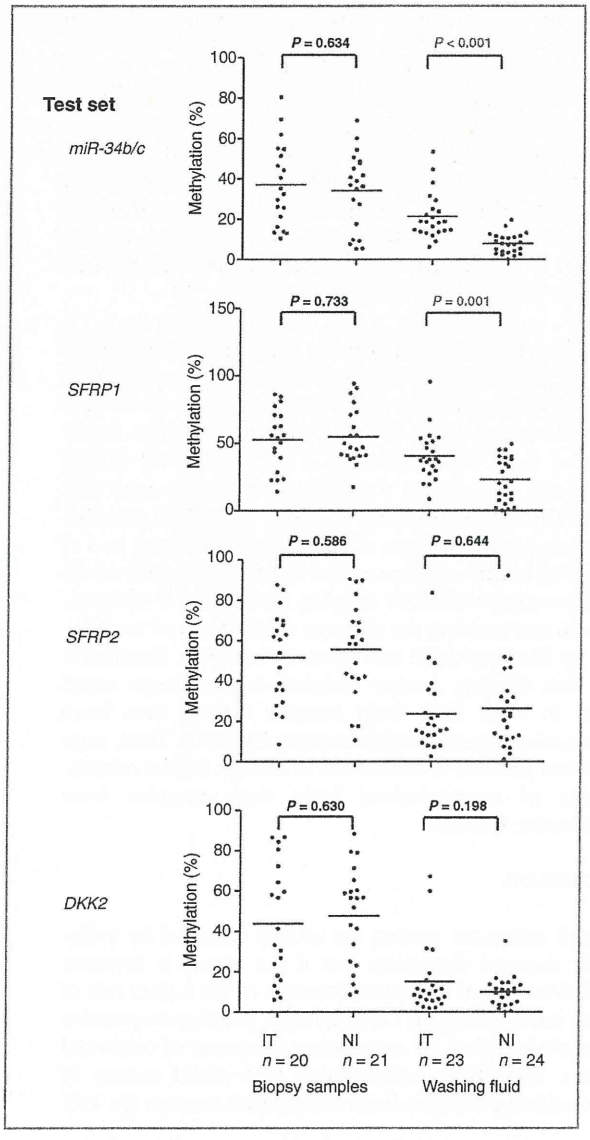

Figure 2. Methylation levels of *mir-34b/c*, *SFRP1*, *SFRP2*, and *DKK2* in the test set. Methylation levels detected with DNA from biopsy tissues and wash fluid. The genes analyzed are shown on the left.

However, invasive colorectal tumors show a heterogeneous pit pattern, making it difficult to determine a therapeutic strategy based on pit pattern diagnosis alone (29). Notably, surface mucus is washed away during magnifying endoscopic analysis, so that utilization of the wash fluid could be an effective noninvasive approach to diagnosis. It has been recommended that nearly all colorectal cancer patients who receive EMR receive periodic endoscopy for early detection of relapses (30). Examination of the methylation levels in the wash fluid could provide helpful information as to how often the patient should receive the follow-up endoscopy (e.g., the lower the methylation level, the less frequently endoscopic examination may be needed). In addition, although we did not include follow-up in our study, it is possible that wash fluid analysis could help physicians detect mucosal relapse after EMR during follow-up endoscopy.

It has been reported that DNA methylation in wash fluid containing pancreatic juice, saliva, or gastric juice is useful for diagnosis and risk assessment in cancer (34–36). For example, Watanabe and colleagues reported that DNA methylation in gastric wash fluid is useful for detection of early gastric cancer (36). The unique feature of our study is that it suggests DNA methylation in colon mucosal wash fluid can be used to predict the invasiveness of tumors. Further study will be necessary to determine whether DNA methylation of colon mucosal wash might also be useful for screening or risk assessment in cancer.

Here we showed that levels of *mir-34b/c* gene methylation were predictive of the invasiveness of colorectal tumors (Figs. 3 and 4; Tables 3 and 4). The sensitivity (0.833) and specificity (0.765) of this approach (well balanced cutoff), as well as the ROC AUC value (0.796), suggest methylation of this gene in colonoscopic wash fluid is a good molecular marker that distinguishes invasive from noninvasive colorectal tumors. We also showed that a diagnostic tree constructed by the combination of methylation levels was highly accurate for predicting invasiveness. To avoid unneeded surgery, it is important that the prediction of invasiveness is highly specific. In this regard, the specificities of the diagnostic tree were 0.882 in the training set, and 0.958 in the test set.

There is currently no molecular test that distinguishes invasive from noninvasive colorectal tumors. DNA methylation can be used as a biomarker for detection of colorectal lesions (16–20), but genes frequently methylated in cancer are also frequently methylated in early lesions (e.g., adenomas), and even in normal colorectal mucosa from aged patients (21, 22). It is therefore difficult to distinguish invasive tumors from noninvasive ones. We previously showed that *SFRP1* and *SFRP2* are frequently methylated in colorectal cancer (28). However, they are also often methylated in normal colorectal mucosa in an age-related manner (34), which is consistent with our present findings. The *mir-34b/c* gene is a putative tumor suppressor whose expression is induced by p53 (35). We previously showed that *mir-34b/c* is silenced by DNA methylation in colorectal cancers and adenomas (25). In this study, we found that methylation of *mir-34b/c* in noninvasive tumors is as high as that in invasive tumors. By contrast, levels of *mir-34b/c* methylation in normal colorectal mucosa are low. Thus, given the high frequency of methylation in tumors, tumor-specific methylation of *mir-34b/c* may be a highly useful molecular marker for colorectal cancer.

The molecular mechanism underlying the high levels of DNA methylation in wash fluid from invasive tumors is not fully understood. Analysis of nuclear staining, DNA methylation, and *K-ras* mutation suggest that wash fluid–derived DNA from invasive tumors contains higher concentrations of tumor-derived DNA than wash fluid from

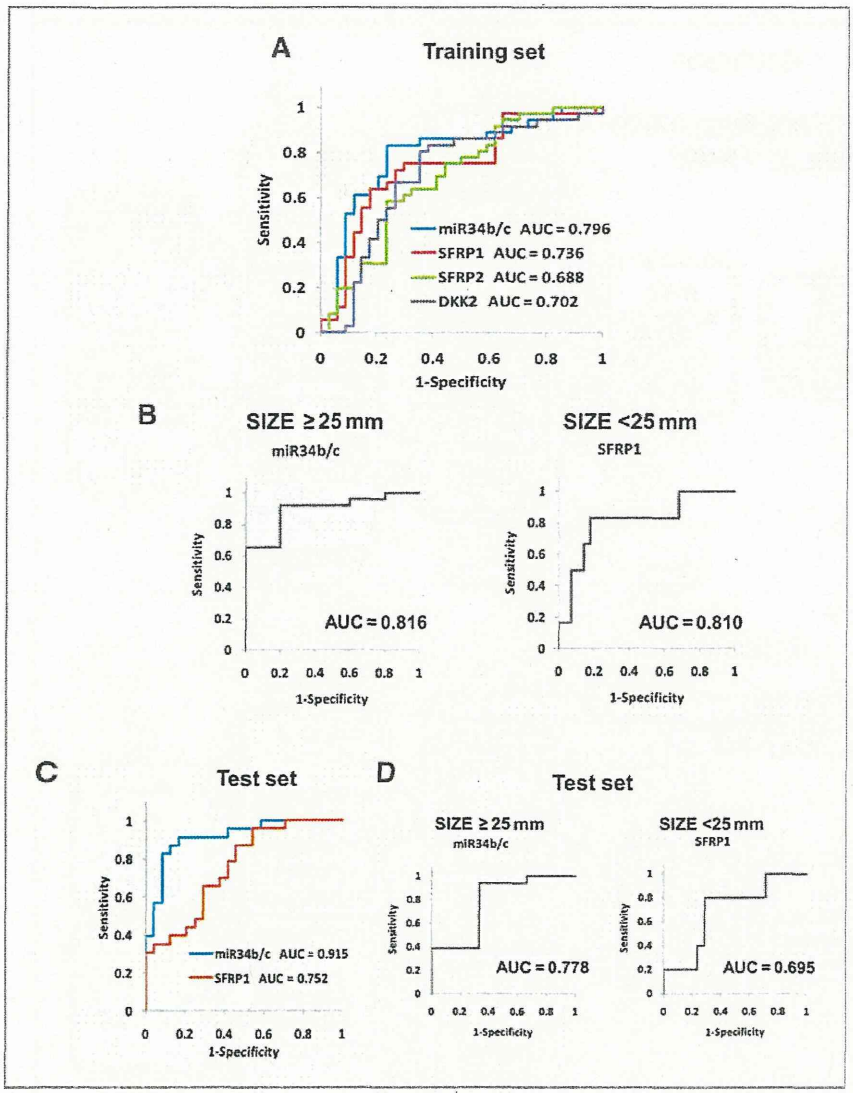

Figure 3. ROC curve analysis. ROC curves were constructed by plotting sensitivity vs. 1-specificity. Curves are shown comparing invasive vs. noninvasive tumors. AUCs are also shown in the graphs. A and B, ROC curve analysis for the training set. Overall analysis is shown in A, and stratified analysis by tumor size (≥25 mm or <25 mm) is shown in B. C and D, the same analysis for the test set. Overall analysis is shown in C, and that stratified by tumor size (≥25 mm or <25 mm) is shown in D.

Table 4. Results of ROC analyses of the methylation levels in 4 genes in the test set.

		Test set				
Tumor size	**Genes**	**AUC Estimate (95% CI)**	**Cutoff (%)**	**Sensitivity Estimate (95% CI)**	**Specificity Estimate (95% CI)**	**ORs Estimate (95% CI)**
Total	*miR34b/c*	0.915 (0.833–0.997)	13.0	0.870 (0.664–0.972)	0.875 (0.676–0.973)	46.7 (8.4–258.9)
			17.8	0.565 (0.345–0.768)	0.958 (0.789–0.999)	29.9 (3.4–260.6)
			21.0	0.348 (0.164–0.573)	1.000 (0.858–1.000)	N/A
	SFRP1	0.752 (0.615–0.889)	45.0	0.348 (0.164–0.573)	0.875 (0.676–0.973)	3.7 (0.8–16.4)
≥25mm	*miR34b/c*	0.778 (0.000–1.000)	15.0	0.667 (0.410–0.867)	0.667 (0.094–0.991)	4.0 (0.3–53.5)
<25mm	*SFRP1*	0.695 (0.450–0.941)	51.0	0.200 (0.005–0.716)	1.000 (0.839–1.000)	N/A

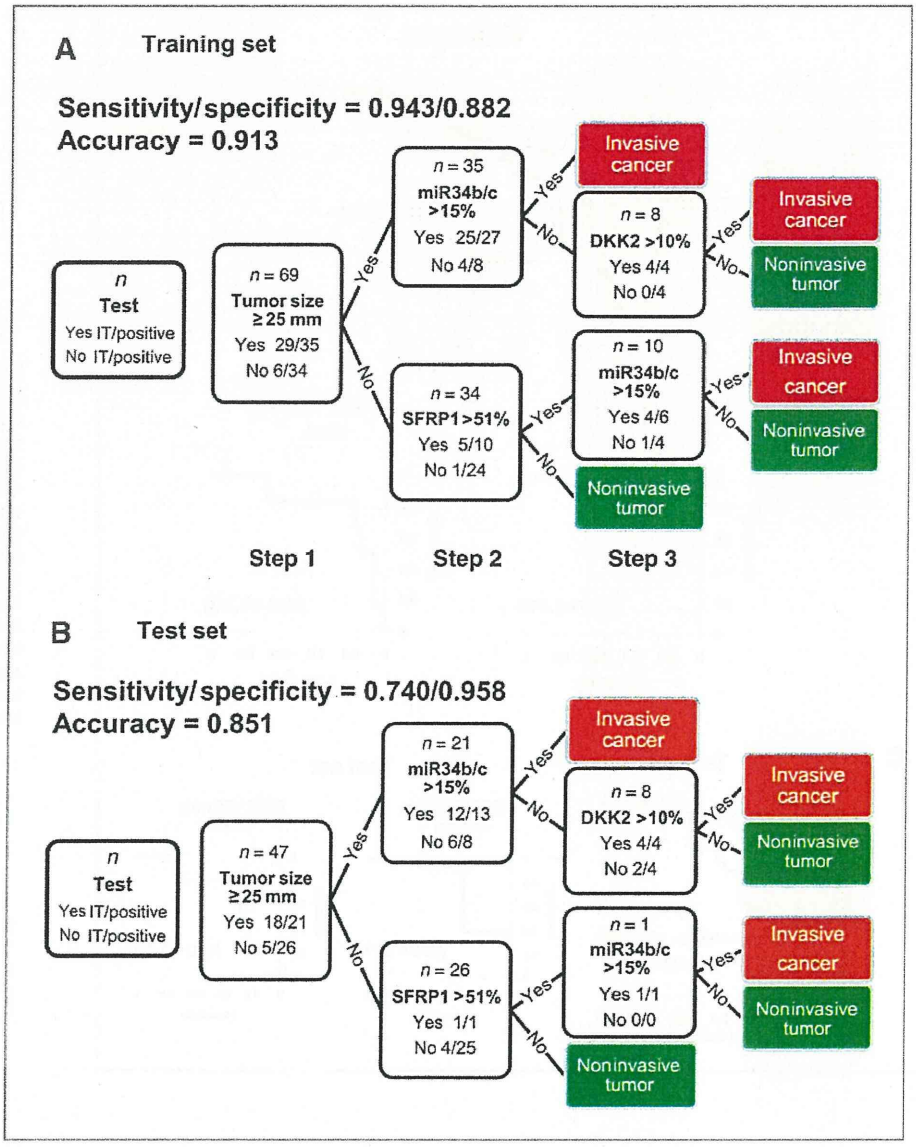

Figure 4. A diagnostic tree to classify invasive and noninvasive tumors on the basis of methylation levels detected in wash fluid. A, a diagnostic tree constructed on the basis of the training set. The majority class in each leaf is the predictive class. B, the application of the diagnostic tree to the test set.

noninvasive tumors. It is generally accepted that colonic epithelial cells are exfoliated into the lumen, that cancer cells can be detected among stool-derived exfoliated cells, and that stool DNA/RNA derived from exfoliated cells may be useful for diagnosis (36, 37). In that context, there are several possible explanations for the higher concentration of DNA from invasive tumor cells in colonoscopy wash fluid. Resistance to apoptosis and loss of cell adhesion are characteristic features of invasive cells (38, 39), which may facilitate the survival of exfoliated cells allowing for good DNA quality. Although we did not detect high levels of methylation in wash fluid from noninvasive tumors, we did obtain relatively large amounts of DNA. The origin of the DNA remains to be determined, but it may be derived from both tumor cells and normal cells such as white blood cells.

Our findings suggest that the high levels of *mir-34b/c* methylation in invasive tumors could be applied to predict invasiveness by using stool DNA. To date, most diagnostic methods for detecting colorectal tumors based on DNA methylation utilize qualitative methylation analysis (16, 19, 20). Using sensitive and quantitative analysis such as BEAMing technology (18), it should be possible to predict the invasiveness of tumors by using stool DNA. Further study to optimize the threshold will be necessary, however.

In summary, high levels of DNA methylation in colorectal washing fluid were correlated with invasiveness of colorectal lesions. Combining endoscopic and DNA

methylation analyses may facilitate accurate preoperative staging of colorectal cancer.

Disclosure of Potential Conflicts of Interest

No potential conflicts of interest were disclosed.

Acknowledgments

The authors thank Dr. William F. Goldman for editing the manuscript.

Grant Support

This study was supported in part by Grants-in-Aid for Scientific Research on Priority Areas (T. Tokino, K. Imai, and M. Toyota), Grants-in-Aid for Scientific Research (S) from the Japan Society for Promotion of Science (K. Imai), a Grant-in-Aid for the Third-term Comprehensive 10-year Strategy for Cancer Control (M. Toyota), and a Grant-in-Aid for Cancer Research from the Ministry of Health, Labor, and Welfare, Japan (M. Toyota).

The costs of publication of this article were defrayed in part by the payment of page charges. This article must therefore be hereby marked *advertisement* in accordance with 18 U.S.C. Section 1734 solely to indicate this fact.

Received August 25, 2010; revised January 19, 2011; accepted January 27, 2011; published online May 4, 2011.

References

1. Jemal A, Siegel R, Ward E, Hao Y, Xu J, Murray T, et al. Cancer statistics, 2008. CA Cancer J Clin 2008;58:71–96.
2. Davies RJ, Miller R, Coleman N. Colorectal cancer screening: prospects for molecular stool analysis. Nat Rev Cancer 2005;5:199–209.
3. Osborn NK, Ahlquist DA. Stool screening for colorectal cancer: molecular approaches. Gastroenterology 2005;128:192–206.
4. Kwok H, Bissett IP, Hill GL. Preoperative staging of rectal cancer. Int J Colorectal Dis 2000;15:9–20.
5. Yamada I, Okabe S, Enomoto M, Sugihara K, Yoshino N, Tetsumura A, et al. Colorectal carcinoma: in vitro evaluation with high-spatial-resolution 3D constructive interference in steady-state MR imaging. Radiology 2008;246:444–53.
6. Hurlstone DP, Cross SS, Adam I, Shorthouse AJ, Brown S, Sanders DS, et al. A prospective clinicopathological and endoscopic evaluation of flat and depressed colorectal lesions in the United Kingdom. Am J Gastroenterol 2003;98:2543–9.
7. Kudo S, Kashida H, Tamura T, Kogure E, Imai Y, Yamano H, et al. Colonoscopic diagnosis and management of nonpolypoid early colorectal cancer. World J Surg 2000;24:1081–90.
8. Soetikno R, Friedland S, Kaltenbach T, Chayama K, Tanaka S. Nonpolypoid (flat and depressed) colorectal neoplasms. Gastroenterology 2006;130:566–76; quiz 88–9.
9. Bianco MA, Rotondano G, Marmo R, Garofano ML, Piscopo R, de Gregorio A, et al. Predictive value of magnification chromoendoscopy for diagnosing invasive neoplasia in nonpolypoid colorectal lesions and stratifying patients for endoscopic resection or surgery. Endoscopy 2006;38:470–6.
10. Matsuda T, Fujii T, Saito Y, Nakajima T, Uraoka T, Kobayashi N, et al. Efficacy of the invasive/non-invasive pattern by magnifying chromoendoscopy to estimate the depth of invasion of early colorectal neoplasms. Am J Gastroenterol 2008;103:2700–6.
11. Kanao H, Tanaka S, Oka S, Hirata M, Yoshida S, Chayama K. Narrow-band imaging magnification predicts the histology and invasion depth of colorectal tumors. Gastrointest Endosc 2009;69:631–6.
12. Markowitz SD, Bertagnolli MM. Molecular origins of cancer: Molecular basis of colorectal cancer. N Engl J Med 2009;361:2449–60.
13. Wong JJ, Hawkins NJ, Ward RL. Colorectal cancer: a model for epigenetic tumorigenesis. Gut 2007;56:140–8.
14. Issa JP. CpG island methylator phenotype in cancer. Nat Rev Cancer 2004;4:988–93.
15. Jones PA, Baylin SB. The epigenomics of cancer. Cell 2007;128:683–92.
16. Glöckner SC, Dhir M, Yi JM, McGarvey KE, Van Neste L, Louwagie J, et al. Methylation of TFPI2 in stool DNA: a potential novel biomarker for the detection of colorectal cancer. Cancer Res 2009;69:4691–9.
17. Hellebrekers DM, Lentjes MH, van den Bosch SM, Melotte V, Wouters KA, Daenen KL, et al. GATA4 and GATA5 are potential tumor suppressors and biomarkers in colorectal cancer. Clin Cancer Res 2009;15:3990–7.
18. Li M, Chen WD, Papadopoulos N, Goodman SN, Bjerregaard NC, Laurberg S, et al. Sensitive digital quantification of DNA methylation in clinical samples. Nat Biotechnol 2009;27:858–63.
19. Müller HM, Oberwalder M, Fiegl H, Morandell M, Goebel G, Zitt M, et al. Methylation changes in faecal DNA: a marker for colorectal cancer screening? Lancet 2004;363:1283–5.
20. Zou HZ, Yu BM, Wang ZW, Sun JY, Cang H, Gao F, et al. Detection of aberrant p16 methylation in the serum of colorectal cancer patients. Clin Cancer Res 2002;8:188–91.
21. Ahuja N, Li Q, Mohan AL, Baylin SB, Issa JP. Aging and DNA methylation in colorectal mucosa and cancer. Cancer Res 1998;58:5489–94.
22. Issa JP, Ottaviano YL, Celano P, Hamilton SR, Davidson NE, Baylin SB. Methylation of the oestrogen receptor CpG island links ageing and neoplasia in human colon. Nat Genet 1994;7:536–40.
23. Park SJ, Rashid A, Lee JH, Kim SG, Hamilton SR, Wu TT. Frequent CpG island methylation in serrated adenomas of the colorectum. Am J Pathol 2003;162:815–22.
24. Satoh A, Toyota M, Itoh F, Sasaki Y, Suzuki H, Ogi K, et al. Epigenetic inactivation of CHFR and sensitivity to microtubule inhibitors in gastric cancer. Cancer Res 2003;63:8606–13.
25. Toyota M, Suzuki H, Sasaki Y, Maruyama R, Imai K, Shinomura Y, et al. Epigenetic silencing of microRNA-34b/c and B-cell translocation gene 4 is associated with CpG island methylation in colorectal cancer. Cancer Res 2008;68:4123–32.
26. Kusano M, Toyota M, Suzuki H, Akino K, Aoki F, Fujita M, et al. Genetic, epigenetic, and clinicopathologic features of gastric carcinomas with the CpG island methylator phenotype and an association with Epstein-Barr virus. Cancer 2006;106:1467–79.
27. Sato H, Suzuki H, Toyota M, Nojima M, Maruyama R, Sasaki S, et al. Frequent epigenetic inactivation of DICKKOPF family genes in human gastrointestinal tumors. Carcinogenesis 2007;28:2459–66.
28. Suzuki H, Watkins DN, Jair KW, Schuebel KE, Markowitz SD, Chen WD, et al. Epigenetic inactivation of SFRP genes allows constitutive WNT signaling in colorectal cancer. Nat Genet 2004;36:417–22.
29. Tanaka S, Kaltenbach T, Chayama K, Soetikno R. High-magnification colonoscopy (with videos). Gastrointest Endosc 2006;64:604–13.
30. Winawer SJ, Zauber AG, Fletcher RH, Stillman JS, O'Brien MJ, Levin B, et al. Guidelines for colonoscopy surveillance after polypectomy: a consensus update by the US Multi-Society Task Force on Colorectal Cancer and the American Cancer Society. Gastroenterology 2006;130:1872–85.
31. Matsubayashi H, Canto M, Sato N, Klein A, Abe T, Yamashita K, et al. DNA methylation alterations in the pancreatic juice of patients with suspected pancreatic disease. Cancer Res 2006;66:1208–17.
32. Pattani KM, Zhang Z, Demokan S, Glazer C, Loyo M, Goodman S, et al. Endothelin receptor type B gene promoter hypermethylation in salivary rinses is independently associated with risk of oral cavity cancer and premalignancy. Cancer Prev Res 2010;3:1093–103.
33. Watanabe Y, Kim HS, Castoro RJ, Chung W, Estecio MR, Kondo K, et al. Sensitive and specific detection of early gastric cancer with DNA methylation analysis of gastric washes. Gastroenterology 2009;136:2149–58.

34. Shen L, Toyota M, Kondo Y, Lin E, Zhang L, Guo Y, et al. Integrated genetic and epigenetic analysis identifies three different subclasses of colon cancer. Proc Natl Acad Sci U S A 2007;104:18654–9.
35. He L, He X, Lim LP, de Stanchina E, Xuan Z, Liang Y, et al. A microRNA component of the p53 tumour suppressor network. Nature 2007; 447:1130–4.
36. White V, Scarpini C, Barbosa-Morais NL, Ikelle E, Carter S, Laskey RA, et al. Isolation of stool-derived mucus provides a high yield of colonocytes suitable for early detection of colorectal carcinoma. Cancer Epidemiol Biomarkers Prev 2009;18:2006–13.
37. Zhao C, Ivanov I, Dougherty ER, Hartman TJ, Lanza E, Bobe G, et al. Noninvasive detection of candidate molecular biomarkers in subjects with a history of insulin resistance and colorectal adenomas. Cancer Prev Res 2009;2:590–7.
38. Brown JM, Attardi LD. The role of apoptosis in cancer development and treatment response. Nat Rev Cancer 2005;5: 231–7.
39. Christofori G. Changing neighbours, changing behaviour: cell adhesion molecule-mediated signalling during tumour progression. EMBO J 2003;22:2318–23.

Carcinogenesis vol.31 no.3 pp.342–349, 2010
doi:10.1093/carcin/bgp179
Advance Access publication July 28, 2009

IGFBP7 is a p53-responsive gene specifically silenced in colorectal cancer with CpG island methylator phenotype

Hiromu Suzuki[1,2,3], Shinichi Igarashi[1], Masanori Nojima[4], Reo Maruyama[1], Eiichiro Yamamoto[1], Masahiro Kai[2], Hirofumi Akashi[5], Yoshiyuki Watanabe[6], Hiroyuki Yamamoto[1], Yasushi Sasaki[3], Fumio Itoh[6], Kohzoh Imai[1], Tamotsu Sugai[7], Lanlan Shen[8], Jean-Pierre J.Issa[8], Yasuhisa Shinomura[1], Takashi Tokino[3] and Minoru Toyota[2,*]

[1]First Department of Internal Medicine, [2]Department of Biochemistry, [3]Department of Molecular Biology, Cancer Research Institute, [4]Department of Public Health and [5]Center for Bioinformation, Sapporo Medical University, South 1,West 17, Chuo-ku, Sapporo 060-8556, Japan, [6]Department of Gastroenterology and Hepatology, St Marianna University School of Medicine, Kawasaki 216-8511, Japan, [7]Division of Diagnostic Molecular Pathology, Department of Pathology, Iwate Medical University, Morioka 020-8505, Japan and [8]Department of Leukemia and Epigenetics Center, University of Texas M. D. Anderson Cancer Center, Houston, TX 77030, USA

*To whom correspondence should be addressed. Tel: +81 11 611 2111 ext. 2680; Fax: +81 11 622 1918;
Email: mtoyota@sapmed.ac.jp
Correspondence may also be addressed to Yasuhisa Shinomura.
Tel: +81 11 611 2111 ext. 3210; Fax: +81 11 611 2282;
Email: shinomura@sapmed.ac.jp

A subset of colorectal cancers (CRCs) show simultaneous methylation of multiple genes; these tumors have the CpG island methylator phenotype (CIMP). CRCs with CIMP show a specific pattern of genetic alterations, including a high frequency of *BRAF* mutations and a low frequency of *p53* mutations. We therefore hypothesized that genes inactivated by DNA methylation are involved in the BRAF- and p53-signaling pathways. Among those, we examined the epigenetic inactivation of insulin-like growth factor-binding protein 7 (*IGFBP7*) expression in CRCs. We found that in CRC cell lines, the silencing of *IGFBP7* expression was correlated with high levels of DNA methylation and low levels of histone H3K4 methylation. Luciferase and chromatin immunoprecipitation assays in unmethylated cells revealed that p53 induces expression of *IGFBP7* upon binding to a p53 response element within intron 1 of the gene. Treating methylated CRC cell lines with 5-aza-2′-deoxycytidine restored p53-induced *IGFBP7* expression. Levels of *IGFBP7* methylation were also significantly higher in primary CRC specimens than in normal colonic tissue ($P < 0.001$). Methylation of *IGFBP7* was correlated with BRAF mutations, an absence of p53 mutations and the presence of CIMP. Thus, epigenetic inactivation of *IGFBP7* appears to play a key role in tumorigenesis of CRCs with CIMP by enabling escape from p53-induced senescence.

Introduction

Colorectal cancer (CRC) arises through the accumulation of multiple genetic changes, including mutation of *APC*, *K-ras* and *p53* (1). In addition to genetic changes, however, epigenetic alterations such as DNA methylation also play a role through the silencing of cancer-related genes (2–4). Moreover, a subset of CRCs show methylation of multiple genes, which has been termed the CpG island methylator phenotype (CIMP, ref. 5). Tumors with CIMP show distinct pattern of genetic alterations, including a high frequency of *K-ras* and *BRAF* mutations and a low frequency of *p53* mutations (6–8). The molecular mechanism underlying this pattern of mutations remains unknown.

Senescence is a state of permanent growth arrest in which cells are refractory to mitogenic stimuli. Although activation of Ras exerts a mitogenic effect in immortalized cells, expression of oncogenic Ras provokes stress responses in primary cells that results in irreversible growth arrest termed premature senescence (9,10). In most cell types, activation of p53 is crucial for initiating senescence in response to DNA damage, and it has been shown that p53-mediated senescence is caused by induction of target genes such as *p21WAF1/CDKN1A*, *PAI-1* and *DEC-1* (11,12).

p53 is a transcription factor that induces expression of various genes involved in cell cycle checkpoints, apoptosis and DNA repair (13), and a variety of approaches, including differential display, representational difference analysis and complementary DNA (cDNA) microarray, have been used to identify its targets. p53 acts by binding to so-called p53 response elements (p53REs), which consist of two copies of a 10 bp motif, separated by 0–12 bp. Using the p53RE as a probe, we previously employed an in silico approach to identify the vitamin D receptor gene as a transcriptional target of p53 (14), which confirmed the utility of the in silico analysis for identification of p53 target genes within the human genome.

Insulin-like growth factor-binding protein 7 (IGFBP7; also called IGFBP-r1 or MAC25) can inhibit proliferation of cancer cells, and its expression is downregulated in various types of tumors (15,16). For instance, *IGFBP7* is silenced by DNA methylation in both colorectal and gastric cancers (17,18). Although the function of IGFBP7 in tumorigenesis is not fully understood, Wajapeyee *et al.* (19) recently reported that expression of activated BRAF in primary melanocytes leads to synthesis of IGFBP7, which then acts through autocrine/paracrine pathways to inhibit extracellular signal-regulated kinase signaling and induce senescence and apoptosis in BRAF-activated cells. Our findings in the present study indicate that *IGFBP7* is a direct target of p53, suggesting that IGFBP7 is a mediator of p53-dependent growth suppression and that epigenetic inactivation of *IGFBP7* is a potentially useful molecular target for the diagnosis and treatment of CRCs with CIMP.

Abbreviations: ADR, adriamycin; cDNA, complementary DNA; ChIP, chromatin immunoprecipitation; CIMP, CpG island methylator phenotype; CRC, colorectal cancer; DAC, 5-aza-2′-deoxycytidine; DNMT1, DNA methyltransferase 1; IGFBP7, insulin-like growth factor-binding protein 7; mRNA, messenger RNA; MSP, methylation-specific polymerase chain reaction; PCR, polymerase chain reaction; p53RE, p53 response element.

Materials and methods

Cell lines and tissue specimens

A set of nine CRC cell lines (CaCO2, Colo320, DLD1, HCT116, HT29, LoVo, RKO, SW48 and SW480) and a lung cancer cell line (H1299) were obtained and cultured as described previously (14,20). HCT116 cells harboring genetic disruptions within the *DNA methyltransferase 1 (DNMT1)* and *DNMT3B* loci (DKO2) (21) and within the *TP53* locus (22) have been described previously. A total of 87 primary CRCs, 49 colorectal adenoma and 41 normal colon specimens were collected as described previously (7). Informed consent was obtained from all patients before collection of the specimens. Genomic DNA was extracted using the standard phenol–chloroform procedure. Total RNA was extracted using TRIZOL reagent (Invitrogen, Carlsbad, CA) and then treated with a DNA-free kit (Ambion, Austin, TX). Genomic DNA and total RNA from normal colon tissue from a healthy individual were purchased from BioChain (Hayward, CA).

Drug treatment

To analyze restoration of *IGFBP7* gene expression, CRC cells were treated with 2 μM 5-aza-2′-deoxycytidine (DAC) (Sigma, St Louis, MO) for 72 h, replacing the drug and medium every 24 h. To determine whether *IGFBP7* is upregulated by endogenous p53, wild-type and $p53^{-/-}$ HCT116 cells were treated with 0.1 μM DAC for 48 h, replacing the drug and medium 24 h after the beginning of treatment. This was followed by addition of adriamycin (ADR) to a final concentration of 0.5 μg/ml and incubation for an additional 24 h.

In silico identification of p53RE

A p53RE database was created as described previously (14). Briefly, human genome sequence data were downloaded from the National Center for

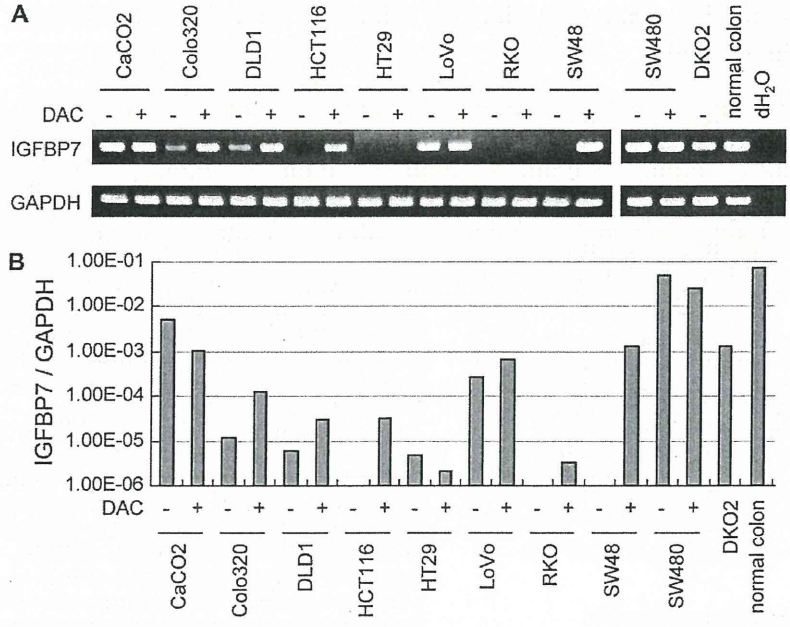

Fig. 1. Analysis of *IGFBP7* expression in CRC cell lines. (**A**) Reverse transcriptase–PCR analysis of *IGFBP7* in the indicated CRC cell lines. Expression of *IGFBP7* was examined using cDNA prepared from CRC cell lines treated with mock (−) or 1.0 μM DAC (+). Glyceraldehyde-3-phosphate dehydrogenase (GAPDH) expression was used as a control to confirm the integrity of the RNA. (**B**) Real-time PCR analysis of *IGFBP7*. The results were normalized using levels of glyceraldehyde-3-phosphate dehydrogenase expression as control.

Biotechnology Information Human Assembly 33. Stored in the p53RE database were sequences containing fewer than four mismatches in the 20 nucleotide p53RE consensus sequence and a spacer of fewer than 12 bp between the two 10 bp motifs. We then analyzed the distribution of p53REs with respect to transcription start sites for *IGFBP7*, taking into consideration the number of mismatches and the length of the spacers.

Reverse transcriptase–polymerase chain reaction

Single-stranded cDNA was prepared using SuperScript III reverse transcriptase (Invitrogen), and the integrity of the cDNA was confirmed by amplifying glyceraldehyde-3-phosphate dehydrogenase (*GAPDH*). Polymerase chain reaction (PCR) was run in a 50 μl volume containing 100 ng of cDNA, 1× Ex Taq Buffer (TaKaRa, Otsu, Japan), 0.3 mM deoxynucleoside triphosphate, 0.25 μM each primer and 1 U of TaKaRa Ex Taq Hot Start Version (TaKaRa). The PCR protocol entailed 5 min at 95°C; 35 cycles of 1 min at 95°C, 1 min at 55°C and 1 min at 72°C; and a 7 min final extension at 72°C. Primer sequences and PCR product sizes are shown in supplementary Table 1 (available at *Carcinogenesis* Online).

Real-time reverse transcriptase–PCR

Real-time reverse transcriptase–PCR was carried out using TaqMan Gene Expression Assays (Applied Biosystems, Carlsbad, CA) and 7900HT Fast Real-Time PCR System (Applied Biosystems) according to the manufacturer's instructions. SDS2.2.2 software (Applied Biosystems) was used for comparative ΔCt analysis, and *GAPDH* served as an endogenous control.

Methylation analysis

Genomic DNA (2 μg) was modified with sodium bisulfite using an EpiTect Bisulfite Kit (Qiagen, Hilden, Germany). Methylation-specific polymerase chain reaction (MSP) and bisulfite sequencing analysis were performed as described previously (23). Bisulfite sequencing and PCR products were cloned into pCR2.1-TOPO vector (Invitrogen), and 8–12 clones from each sample were sequenced using an ABI3130x automated sequencer (Applied Biosystems).

Bisulfite pyrosequencing was carried out as described previously (20) using primers designed with PSQ Assay Design software (Biotage, Uppsala, Sweden). After PCR, the biotinylated products were purified, made single stranded and used as a template in the pyrosequencing reaction run according to the manufacturer's instructions. The PCR products were bound to Streptavidin Sepharose beads HP (Amersham Biosciences, Piscataway, NJ), after which beads containing the immobilized PCR product were purified, washed and denatured using a 0.2 M NaOH solution. After addition of 0.3 μM sequencing primer to the purified PCR product, pyrosequencing was carried out using a PSQ96MA system (Biotage) and Pyro Q-CpG software (Biotage). Primer sequences and PCR product sizes are shown in supplementary Table 1 (available at *Carcinogenesis* Online).

Chromatin immunoprecipitation

Chromatin immunoprecipitation (ChIP) was carried out using a ChIP Assay Kit (Upstate Biotechnology, Lake Placid, NY) with anti-trimethylated histone H3K4 monoclonal antibody (clone MC315; Upstate, Lake Placid, NY) or anti-human p53 monoclonal antibody (DO-1; Santa Cruz Biotechnology, Santa Cruz, CA) as described previously (14,20,24). For histone methylation analysis, HCT116 cells treated with or without DAC and DKO2 cells were used as described previously (20). For p53 analysis, DLD1 cells infected with recombinant adenovirus Ad-p53 or Ad-LacZ were used (14). Briefly, the protein and DNA in 2×10^6 cells were cross-linked in a 1% formaldehyde solution for 15 min at 37°C. The cells were then lysed in 200 μl of sodium dodecyl sulfate lysis buffer and sonicated to generate 300–800 bp DNA fragments. After centrifugation, the cleared supernatant was diluted 10-fold with ChIP dilution buffer, after which one-fiftieth of the extract volume was used for PCR amplification as the input control. The remaining extract was incubated with specific antibody for 16 h at 4°C. Immune complexes were precipitated, washed and eluted as recommended. DNA–protein cross-links were reversed by heating for 4 h at 65°C, after which the DNA fragments were purified and dissolved in 50 μl of Tris–ethylenediaminetetraacetic acid. One microliter of each sample was used as a template for PCR amplification. Real-time PCR for histone analysis was carried as described previously (20) using the primers listed in supplementary Table 1 (available at *Carcinogenesis* Online). PCR amplification of *IGFBP7* containing the putative p53RE was also carried out using primers listed in supplementary Table 1 (available at *Carcinogenesis* Online).

Luciferase assays

Reporter plasmids pGL3-RE-*IGFBP7* and pGL3-RE-*IGFBP7*-mut were constructed as follows. Three tandem repeats of RE-*IGFBP7* (5′-AAACAAGTCCAAGCTTGCTG-3′) and its unresponsive mutant form, RE-*IGFBP7*-mut (5′-AAAAAATTCCAAGATTTCTG-3′), were synthesized and inserted upstream of a basal SV40 promoter in the pGL3-promoter vector (Promega, Madison, WI), yielding pGL3-RE-*IGFBP7* and pGL3-RE-*IGFBP7*-mut, respectively. Using Lipofectamine 2000 (Invitrogen), H1299 cells (5×10^4 cells per well in 24-well plates) were transfected with 100 ng of one of the reporter plasmids, 100 ng of pcDNA-p53 or an empty vector and 2 ng of pRL-TK (Promega). Luciferase activities were measured 48 h after transfection using a Dual-Luciferase Reporter Assay System (Promega). The ability to stimulate transcription was determined

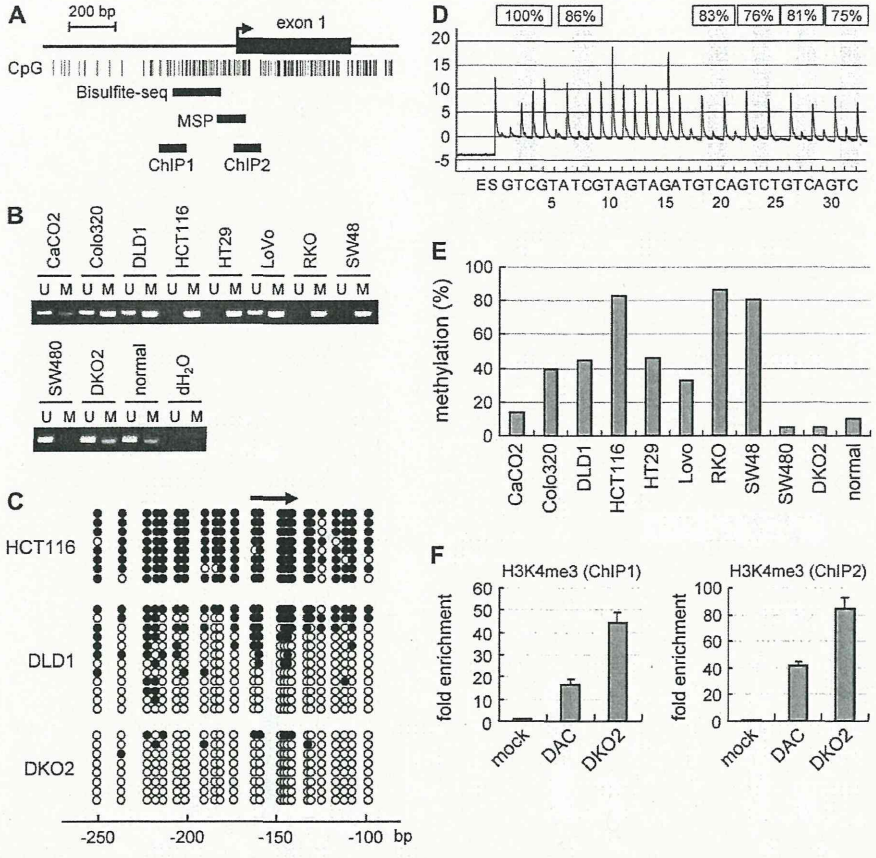

Fig. 2. Methylation analysis of *IGFBP7*. (**A**) Schematic representation of the 5′ region of *IGFBP7*. CpG sites are shown as vertical bars. The regions analyzed by bisulfite sequencing, MSP and ChIP are indicated by solid bars. The transcription start site is indicated by an arrow. (**B**) MSP analysis of *IGFBP7* in CRC cell lines. The cell lines examined are shown on the top. (**C**) Bisulfite sequencing of IGFBP7. Open and filled circles represent unmethylated and methylated CpG sites, respectively. (**D**) Representative pyrogram for *IGFBP7*. Gray columns indicate regions with C to T polymorphic sites. The percentage of methylation at each CpG site is shown at the top; *y*-axis, signal peaks proportional to the number of nucleotides incorporated and *x*-axis, the nucleotides incorporated. (**E**) Summary of pyrosequencing. *y*-axis, the percentages of methylated cytosines in the samples, as determined from pyrosequencing. (**F**) ChIP analysis of trimethylation of histone H3K4 in the 5′ region of IGFBP7. ChIP assays were performed using HCT116 cells treated with mock or DAC. DKO2 cells (*DNMT1*$^{-/-}$*DNMT3B*$^{-/-}$ HCT116 cells) were also used.

from the ratio of luciferase activity in the cells transfected with the pGL3-RE-*IGFBP7* to the activity in the cells transfected with pGL3-RE-*IGFBP7*-mut. All experiments were performed in triplicate and repeated at least three times.

Expression vector

Full-length *IGFBP7* cDNA was PCR amplified using cDNA derived from DKO2 cells as a template. The PCR was run in a 50 μl volume containing 1× AccuPrime *Pfx* Reaction mix (Invitrogen), 0.3 μM each primer and 2.5 U of AccuPrime *Pfx* DNA polymerase (Invitrogen). The PCR protocol entailed 2 min at 95°C; 35 cycles of 15 s at 95°C, 30 s at 62°C and 1 min at 68°C; and a 5 min final extension at 68°C. Primer sequences are listed in supplementary Table 1 (available at *Carcinogenesis* Online). Amplified PCR products were then incubated with 1 U of Ex Taq DNA Polymerase (TaKaRa) for 10 min and cloned into pCR2.1-TOPO (Invitrogen). After the sequences were verified, fragments were cut using EcoRI and ligated into EcoRI-digested pcDNA3.1/HisA (Invitrogen).

Colony formation assays

Colony formation assays were carried out as described previously (25). Briefly, cells (1×10^5 cells) were transfected with 5 μg of one of the pcDNA3.1His-IGFBP7 vectors or with empty vector using Lipofectamine 2000 according to the manufacturer's instructions. Cells were then plated on 60 mm culture dishes and selected for 14 days with 0.6 mg/ml G418, after which the colonies that formed were stained with Giemsa and counted using National Institutes of Health IMAGE software.

Statistics

Statistical analyses were carried out using SPSSJ 15.0 (SPSS Japan, Tokyo, Japan). Pearson's correlation coefficient and *t*-test were used to evaluate the association between *IGFBP7* methylation. Methylation of *p16*, mutations of *p53*, mutations of *BRAF*, microsatellite instability and CIMP status were determined as described previously (5,7,26). Values of $P < 0.05$ were considered significant. To identify potentially distinct subgroups among colon cancer and adenoma patients, heat maps were constructed using K-means clustering method (27).

Results

Analysis of IGFBP7 expression in CRC cell lines

To test whether *IGFBP7* is epigenetically silenced in CRC, we first carried out an reverse transcriptase–PCR analysis with a set of CRC cell lines. We found that expression of *IGFBP7* messenger RNA (mRNA) was completely absent in four of the nine cell lines tested (HCT116, HT29, RKO and SW48) and was downregulated in two cell lines (Colo320 and DLD1) (Figure 1A). In many of the cells in which *IGFBP7* was downregulated, treatment with the DNA methyltransferase inhibitor DAC rapidly restored mRNA expression, which is indicative of epigenetic silencing of the genes through DNA methylation (Figure 1A). We also analyzed HCT116 cells in which the DNA methyltransferase genes *DNMT1* and *DNMT3B* were genetically disrupted (DKO2 cells), thereby abrogating DNA methylation (21). Those cells showed substantially greater expression of *IGFBP7* mRNA than the parental HCT116 cells (Figure 1A). In contrast to the cancer cells, *IGFBP7* was well expressed in normal colonic mucosa from a healthy individual (Figure 1A).